DETERMINATION OF ANTHROPOGENIC CONTAMINATION IN SOIL PROFILES IN THE GEOLOGICALLY ANOMALOUS LANDSCAPE OF NORTHWESTERN BOHEMIA

SLAVOMÍR ADAMEC[1*], ŠTĚPÁNKA TŮMOVÁ[1,2], MAVRO LUCIĆ[3], MICHAL HOŠEK[1,2], TOMÁŠ M. GRYGAR[1,2] (*corresponding author)

[1]Faculty of Environment, Jan Evangelista Purkyně University in Ústí nad Labem, Pasteurova 3632/15, 400 96 Ústí nad Labem, Czech Republic
[2]*Institute of Inorganic Chemistry AS CR, 250 68 Husinec - Řež, Czech Republic*
[3]*Ruđer Bošković Institute, Department for Marine and Environmental Research, Bijenička cesta 54, 10000 Zagreb, Croatia*

INTRODUCTION

The area of northwestern Bohemia is known for great geological diversity **(Fig.2)** and also for its changes caused by extensive anthropogenic activities in the past **(Fig.1).** Agricultural land in that area has elevated concentrations of some risk elements (e.g. arsenic or beryllium), however, it is not clear if these have resulted from anthropogenic contamination or from natural anomalies in the bedrock. Contamination of NW Bohemia can come from both ore mining and processing and coal mining and combustion. In the case of coal mining and utilization, contamination by atmospheric fallout (As, Cd, Sb) regardless of the bedrock, while contamination from ore mining and processing (As, Sb) can be expected to have smaller spatial impact around historical mines and smelters. Both should increase upward in soil profiles.

MATERIALS AND METHODS

So far, several dozen profiles have been sampled in the Teplice region and in the Ore Mountains and the reference locality NW of Lovosice **(Fig.1)**. The analytical methods in this work include acid extractions and analysis by ICP-MS, as well as total analyses by XRF. ICP MS: : Soil samples (size fraction < 2 mm, 0.5 g) was extracted by 6 ml HCl and 2 ml HNO3 in a Multiwave 5000 microwave (Anton Paar) using European standard “EN ISO 54321:2021: Soil, treated biowaste, sludge and waste - Digestion of aqua regia soluble fractions of elements". The supernatant after centrifugation was diluted and analysed using an ICP-MS Agilent 7900. XRF: Soils samples (< 2 mm) were pulverised in planetary micromill, poured into nylon cells with Mylar foil bottoms and subjected to XRF analysis using an Epsilon 3^X spectrometer (PANalytical, the Netherlands).

AIM

The aim of this work is to distinguish natural contamination from the bedrock and the consequences of anthropogenic activities.

RESULTS

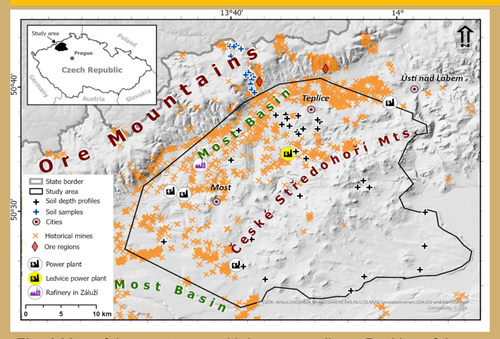

Fig. 1 Map of the target area with its surroundings. Position of the target area in the Czech Republic (inset). Target area includes the Most Basin affected by mining activities in north-west and agricultural areas in south-east, included for comparison

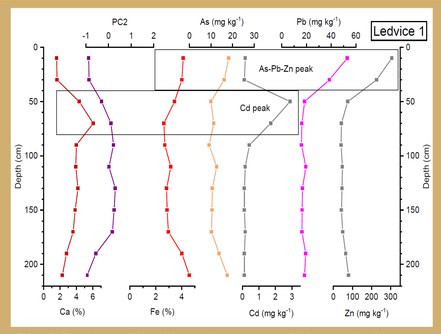

Fig. 3 Depth profile with total contents of lithogenic elements (Ca, PC2, and Fe) and pseudo-total contents of risk elements in the Ledvice village.

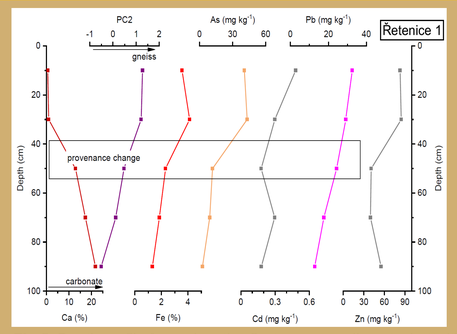

Fig.5 Depth profile formed on the Cretaceous sediments, but with markers of the Ore Mountains soil provenance on top, where also As and Pb contents are considerably increased.

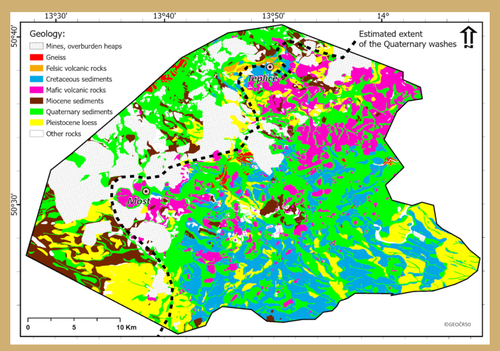

Fig. 2 Simplified geological map with major rock types in the target area. Dashed line shows estimated extent of the Quaternary washes from the Ore Mountains. Dotted white polygons are areas with landscape surface completely altered by coal mining.

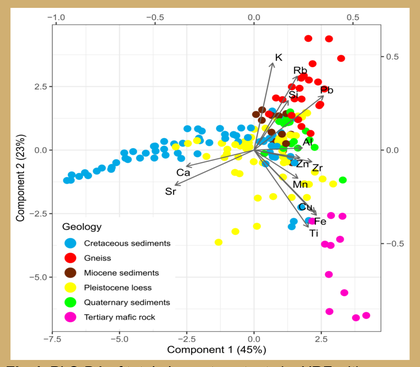

Fig.4 PLS-DA of total element contents by XRF with soil samples post-stratified according to geological map of the bedrocks in sampling sites.

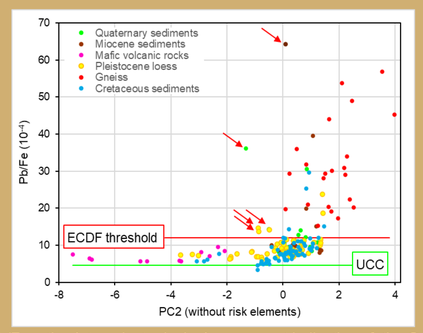

Fig.6 Pb/Fe ratio plot against principal component indicative of the Ore Mountains provenance. Only lithogenic elements were used for PLS-DA. Red arrows indicate Pb contamination not related to the geogenic factors, while most soils with Pb/Fe above the ECDF threshold has high PC2 indicative for the Ore Mountains provenance. Colour coding of soil bedrock is the same as in Fig. 2.

CONCLUSION

Conventional soil mapping, such as RKP (Register of Contaminated Areas) having been performed in the frame of Czech national legislative, can provide valuable preview on the soil contents of risk elements at large spatial scale and coverage of agricultural soils. To obtain this preview at affordable costs, only topsoils are sampled and acid extractions are used in RKP. In the so identified hotspots of soil risk elements, in particular in places where industrial activities have been inherently related to local geogenic anomalies, more detailed sampling and holistic data mining must be employed to separate natural and anthropogenic controls of risk element contents. To achieve this understanding, complete soil depth profiles must be sampled **(Fig.3**, **Fig.5),** equal attention as to risk elements must be paid to lithogenic elements, and soil profiles must be evaluated individually, with respect to the actual local conditions, such as provenance variability and contaminant translocations in soil profiles **(Fig.4, Fig.6)** .The routinely obtained topsoil maps based on RKP thus provide the first step, but then a holistic approach to the individual target areas is needed with methods tailored to the actual local situation. Reliable deciphering of anthropogenic contamination must be based on expert-based approach and understanding to the local specificities.

AKNOWLEDGEMENTS

Authors are grateful to the Ministry of Agriculture of the Czech Republic for providing results from the soil monitoring programme RKP for free for scientific purposes. Karel Mach (North Bohemian Mines) kindly provided scans of the hydrological maps provided kindly by K. Mach (North Bohemian Mines, Bílina), from which the extent of the Quaternary washes from the Ore Mountains to the basin floor were inferred. Part of fieldworks and analyses were funded by student projects UJEP-SGS-44202/15/2084/01, granted to M. Hošek, and another part of those works by student project UJEP-SGS-2023-44-001-2, granted to S. Adamec. The laboratory sample processing and XRF analyses were performed by M. Maříková and P. Vorm in the Institute of Inorganic Chemistry in Řež

ANS 2023

Laboratory of Protein Evolution

A DETAILED IN SILICO ANALYSIS OF THE α-AMYLASE FAMILY GH126 FOCUSED ON ITS UNIQUE SEQUENCE-STRUCTURAL FEATURES

Michaela Schorschová[1] & Štefan Janeček[1,2]

[1] Institute of Biology and Biotechnology, Faculty of Natural Sciences, University of Ss. Cyril and Methodius, Trnava, Slovakia
[2] Laboratory of Protein Evolution, Institute of Molecular Biology, Slovak Academy of Sciences, Bratislava, Slovakia

INTRODUCTION

Glycoside hydrolases (GHs) are important enzymes that catalyze the hydrolysis of glycosidic bonds in carbohydrates [1]. The family GH126 was identified based on a limited biochemical characterization and structural analysis of the amylolytic enzyme CPF_2247 from *Clostridium perfringens* that exhibits the activity on amylose, suggesting its classification as an α-amylase [2]. Interestingly, the GH126 members possess a distinct structure of an $(\alpha/\alpha)_6$-barrel compared to known α-amylases [3] and share a similarity with β-glucan-active enzymes from families GH8 and GH48 of the clan GH-M [2] employing the inverting reaction mechanism [1]. Since α-amylases are α-glucan-active enzymes and use the retaining mechanism, doubts still exist whether or not the family GH126 represents the new α-amylase family in CAZy [3,4].

AIM OF THE STUDY

The main goal of the present study was to undertake a detailed analysis of sequences of the family GH126 available in the CAZy database in an effort to identify their unique sequence-structural features that would distinguish them from both related families GH8 and GH48 of the clan GH-M. The additional aim was to define the conserved sequence regions (CSRs) in the families GH8 and GH48 corresponding to the seven CSRs established in the family GH126 previously [5,6].

Table 1. Selection of sequences .

GH126	Number	Percentage (%)
All sequences	1511	100
Excluded sequences (E)	36	2.38
Redunadant sequences	1297	85.84
Master sequences (M)	74	4.9
Unique sequences (U)	104	6.88
Final set (M + U)	178	11.78

GH8	Number	Percentage (%)
Final set	86	100
Known specificity	69	80.23
Known specificity and structure	13	15.12
Known structure	4	4.65

GH48	Number	Percentage (%)
Final set	66	100
Known specificity	10	15.15
Known specificity and structure	8	12.12
Known structure	3	4.55
Eukaryotic origin	45	68.18

A dataset of 1511 sequences was obtained from the CAZy database in December 2022 with the goal of selecting representative sequences for the target family GH126. The process involved eliminating fragment sequences and those with not unambiguous CSRs and/or substitutions in possible catalytic residues. Finally, 178 GH126 sequences were collected consisting of 104 unique and 74 master (representing 90% identity) sequences (Table 1).

For comparison, similar datasets were prepared for families GH8 and GH48 (supplemented by eukaryotic representatives) from the CAZy database in June 2023; the details being summarized in Table 1.

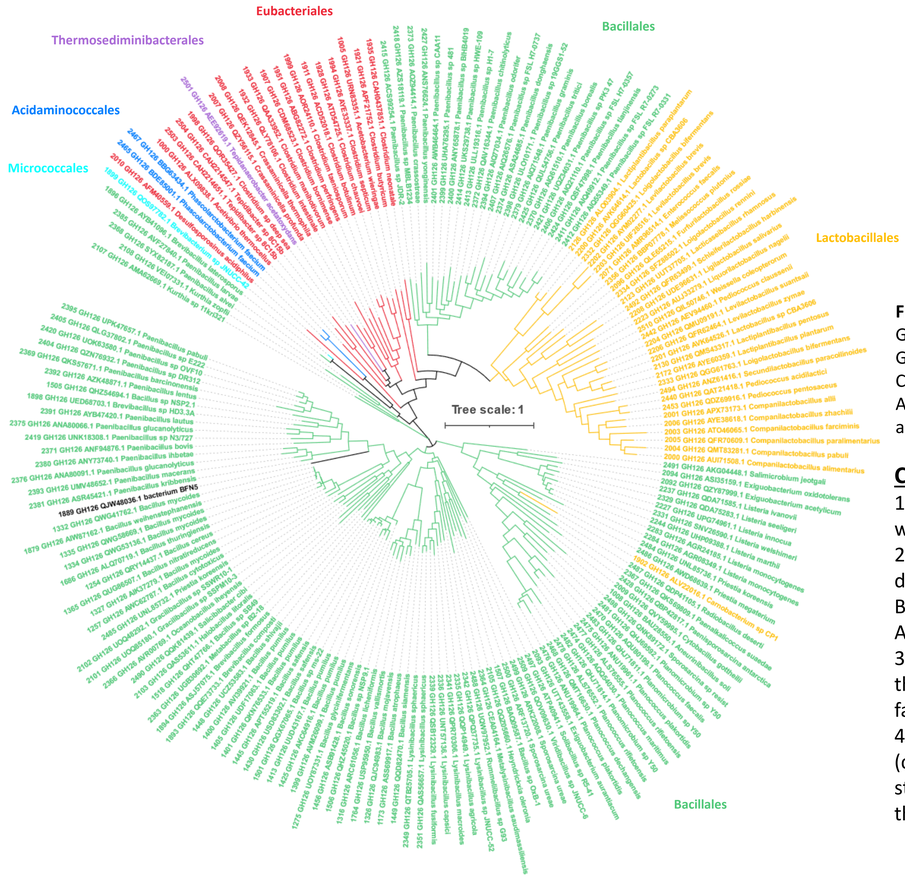

Figure 1. Evolutionary tree showing the order-level taxonomic composition of the family GH126. The tree, based on the alignment of the catalytic domain of 178 family representatives performed with the Clustal-Omega tool, was calculated by the maximum-likelihood method with 500 bootstraps implemented in the MEGA software. The tree was visualized by the i-TOL programme.

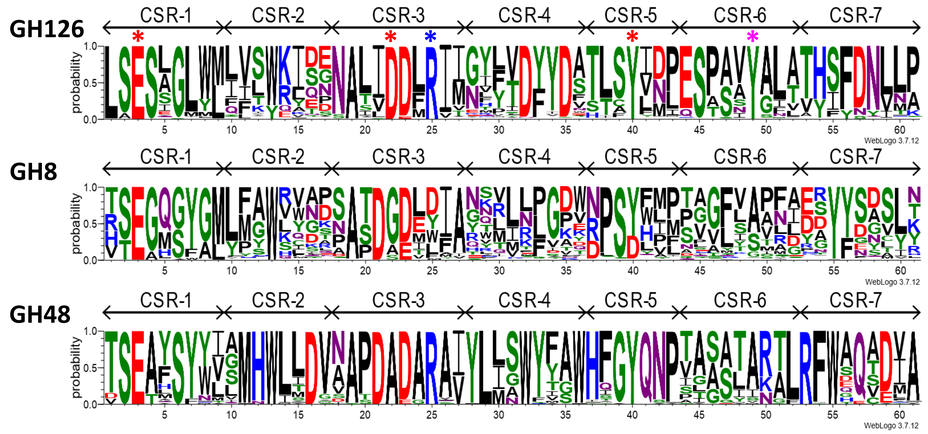

Figure 2. Sequence logos of seven CSRs of the family GH126. The CSRs for families GH8 and GH48 were identified based on the GH126 family's CSRs. The logos for the individual families are based on 1475, 86 and 66 sequences of members of the family GH126, GH8 and GH48, respectively. CSR-1, residues 1–9; CSR-2, residues 10–17; CSR-3, residues 18–27; CSR-4, residues 28–36; CSR-5, residues 37–43; CSR-6, residues 44–52; CSR-7, residues 53–61. Two potential catalytic residues (No. 3 – Glu and No. 22 – Asp) and a functional aromatic residue (No. 40 – Tyr) in the family GH126 are marked by red asterisks. The blue and magenta asterisks signify, respectively, the positions unique for GH126 and GH48 (No. 25. – Arg) and GH126 only (No. 49 – Tyr).

CONCLUSIONS:

1. In the present study, a comprehensive set of sequences was established to represent reliably the family GH126, while characterized sequences belonging to the GH8 and GH48 families were also collected (Table 1).
2. The evolutionary tree (Fig. 1) based on the alignment of catalytic $(\alpha/\alpha)_6$-barrel demonstrated the taxonomic distribution of 178 family GH126 members. The majority of representatives was found as belonging to the Bacillota phylum (formerly known as Firmicutes). Remarkably, one GH126 representative was identified from the Actinomycetota phylum. Additionally, on the taxonomy level, 4 classes, 6 orders and 15 families were recognized.
3. Sequence logos were produced by identifying seven CSRs for all the three studied GH families (Fig. 2). Notably, the logos for families GH126 and GH48 exhibited rather a higher degree of conservation, whereas the logo for the family GH8 displayed interestingly a higher variability.
4. The work in progress covers the finalizing the detailed comparison of both the CSRs and entire sequences of $(\alpha/\alpha)_6$-barrel catalytic domains of GH126, GH8 and GH48 with the aim to reveal and establish the sequence-structural features unique for the family GH126 as well as the elucidating the evolutionary relationships of all the three families GH126, GH8 and GH48 with eventual finding proteins exhibiting the intermediary character.

References:

[1] Drula E., … & Terrapon N (2022) Nucleic Acids Res. 50: D571–D577.
[2] Ficko-Blean E, … & Boraston AB (2011) Proteins 79: 2771–2777.
[3] Janecek S, … & MacGregor EA (2014) Cell. Mol. Life Sci. 71: 1149–1170.
[4] Janecek S & Svensson B (2022) Amylase 6: 1–10.
[5] Kerenyiova L & Janecek S (2020) Carbohydr. Res. 494: 108082.
[6] Kerenyiova L & Janecek S (2020) 3Biotech 10: 420.

Acknowledgment

This work was financially supported by grants FPV10-2023 from the Faculty of Natural Sciences, UCM, Trnava, and 2/0146/21 from the Slovak Grant Agency VEGA.

IDENTIFICATION AND DETERMINATION OF N-NITROSODIMETHYLAMINE (NDMA) AND N-NITROSODIETHYLAMINE (NDEA) IN LOSARTAN BY GC-MS

Anna Jurčová[1], Andrea Lančaričová[1], Andrea Purdešová[2]

[1] Saneca Pharmaceuticals a.s., Nitrianska 100, 920 27 Hlohovec, Slovak Republic

[2] Department of Chemistry, Faculty of Natural Sciences, University of Ss. Cyril and Methodius, J. Herdu 2, 917 01 Trnava, Slovak Republic

INTRODUCTION

Nitrosamines are classified by the ICH M7(R1) Guideline as Class-1 impurities and as "known mutagenic carcinogens", originating from organic synthesis and manufacturing process

Since 2018, regulation and control of genotoxic nitrosamine impurities have been a necessary characteristic of quality and safety of various drugs

In Sartan substances, nitrosamines are formed by reaction of solvent impurities with nitrite ions in the acidic conditions

The acceptance limits of nitrosamine impurities for active pharmaceutical ingredients (API) are 96 ng/day for NDMA and 26.5 ng/day for NDEA

EXPERIMENTAL

Sample preparation

Preparation of sample and extraction of nitrosamines from losartan was conducted according to procedure described in the European Pharmacopoeia (Ph. Eur.) with the modification applied. Both analytes were identified according to NIST database of mass spectrum and quantified according to external standard calibration.

Instrumental analysis

Gas chromatograph SCION 456-GC coupled with the EVOQ GC-TQ from Bruker (Germany), equipped with a PTV (programmable temperature vaporization) injector and an CP-8400 autosampler was operated in the solvent vent mode. The injection volume was 1 µL.

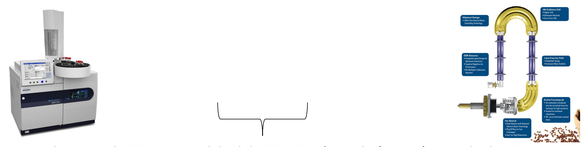

Gas chromatograph SCION 456-GC coupled with the EVOQ GC-TQ from Bruker (Germany), equipped with a PTV (programmable temperature vaporization) injector and an CP-8400 autosampler

AIM

The aim of this study was to identify and quantify two nitrosamine impurities (NDEA and NDMA) in two batches of losartan potassium (losK2104273 and losK111217/NT2) and two batches of losartan base (Losbase 1803358 and 1802713) by sensitive GC-MS procedure

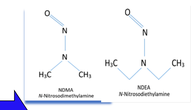

Table 1. Limits of NDMA and NDEA (EMA/409815/2020 Rev.14/2022)

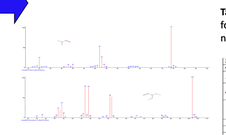

Table 2. Analytical methods for determination of nitrosamines with LOD,LOQ

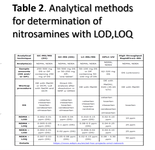

RESULTS

Optimization of the extraction procedure

- The highest solubility of losartan represents 1M sodium hydroxide (according to Ph.Eur. method), in methanol and in mixed solvent (methanol + acetone) was slightly soluble after the lengthy process of sonication and mixing
- Dichloromethane provided high effective extraction of two nitrosamines in term of precision and recovery
- The optimal rate of centrifugation was 5500xg for 10 minutes
- Direct injection of dissolving substance (large amount) in dichloromethane into the inlet of analytical instrument caused presence of interference peaks

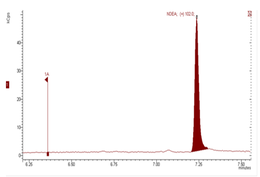

Integrated peak of NDEA in 7.2 minute with the area of 88419 (Batch of Losartan base 1802713) according to SIM mode (ion 102)

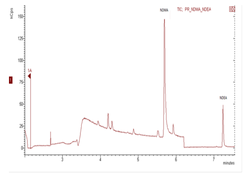

Total ion chromatogram (TIC) of both nitrosamine impurities. Dominant NDMA peak in 5.69 minute and NDEA in 7.20 minute

Method validation

- The validation was performed in the range of 2 ppb (NDEA) and 4 ppb (NDMA) as lower limit of quantification (LLOQ) to 2000 ppb as upper limit of quantification (ULOQ)
- Standard solution and sample solution were stable for 48 hours without change in nitrosamine impurities (change NMT ± 15.0 %)
- Accuracy was determined by addition of reference solution into sample at three concentration levels corresponding to 10 %, 100 % and 120 % of specification limit and met the acceptance limit R = 70 % to 130 %
- Linearity was determined in the range from limit of quantitation to about 150 % of specification limit of both impurities. Eight-point calibration curve showed correlation coefficients higher than 0.99 in both cases
- System precision was evaluated from peak areas of both nitrosamines obtained with consecutive injections of six reference samples. The RSD value of six recoveries of each nitrosamine was less than 15.0 %

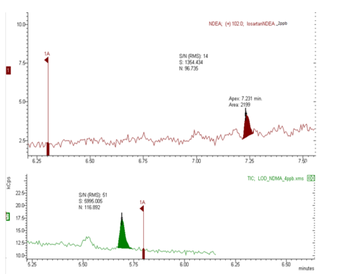

Detection of NDEA and NDMA in trace levels (2.0 ppb and 4.0 ppb)

Table 3. The results of selected parameters of validation and acceptance criteria

Validated parameters	Acceptance criteria	Results
System suitability test System precision	RSD ≤ 15.0 % (n = 6)	NDMA: RSD = 7.94 % NDEA: RSD = 7.51 %
Precision-repeatability	RSD ≤ 15.0 %	NDMA: RSD = 3.78 % NDEA: RSD = 5.11 %
Accuracy - recovery	70 % - 130 % RSD < 15.0 %	NDMA: R = 78 % (average) RSD = 3.99 % NDEA: R = 86 % (average) RSD = 3.85 %
Linearity	r ≥ 0.98	NDMA: r = 0.994 NDEA: r = 0.999
Limit of quantification **Limit of detection**	LOQ ≤ 1/10 of specification limit to be determined	NDMA: LOQ = 0.0960 ppm; RSD = 3.60 % LOD = 4 ppb NDEA: LOQ = 0.0265 ppm; RSD = 3.59 % LOD = 2 ppb
Content of nitrosamines in samples	to be determined	Losartan potassium: NDMA, NDEA - not detected (ND) Losartan base: batch No. 1803358 - NDMA (0.62 ppm) - NDEA (0.73 ppm) RSD = 0.05 % Losartan base: batch No. 1802713 -NDMA (0.13 ppm) -NDEA (0.30 ppm) RSD = 0.06 %
Stability of solutions	change NMT ± 15.0 %	standard and sample solution: stable at least for 48 hours

CONCLUSION

- Nitrosamine impurities present potentially negative consequences for health of patients and is unreliable to monitor the risk of formation of nitrosamines in APIs
- Modified and validated Ph.Eur. method was used in this study and met acceptance criteria according to Q2(R1) ICH guideline
- Dichloromethane was evaluated as optimal elution solvent for extraction of nitrosamines in losartan substances
- Nitrosamines were not detected in batches of losartan potassium. On the other hand, nitrosoamines were quantified in samples of losartan base with values exceeding the acceptance limit

Magnetoactive complexes containing bioactive ligands. A theoretical study

Michaela Červeňáková and Ján Titiš

Institute of Chemistry and Environmental Sciences, University of SS Cyril and Methodius, 91701 Trnava, Slovakia

INTRODUCTION

Based on the current literature, we can state that transition metal complexes represent highly variable structures, which is reflected in its various properties, modulated by the central atom and the ligands. This makes them particularly useful for a variety of applications.

Due to the aforementioned properties of transition metals complexes, including their molecular geometry, redox and catalytic reactions, thermodynamic characteristics, coordination numbers, as well as their ligand exchange and binding with different type of ligands, give them the potential to react and interact with biomolecules and biological systems in different mechanisms. Such interactions of the metals with various biomolecules, especially nucleic acids, proteins, enzymes, etc., lead to their extensive use for potential therapeutic purposes, which include antibacterial, antiviral, antifungal, anti-inflammatory and antitumor properties. Because the DNA molecule, due to its unique structure, size, conformations, and complexity, provides a large number of potential binding sites, coordination transition metal compounds can bind to DNA in two ways of interaction: covalent and non-covalent binding. The covalent binding involves the interaction of the central metal ion with the nitrogenous base or phosphate group of the DNA molecule chain. The predominant mode of metal interaction takes place in the case of guanine at N7 and O6, in the case of adenine bases it is N7 and N1, in the case of pyrimidines it is N3. In this binding method, the labile part of the given complex is replaced by the nitrogenous base of the DNA molecule. An example can be a guanine N7 in cisplatin, which inhibits DNA replication and cell death. In the case of a non-covalent of interaction, we distinguish three methods: intercalation, electrostatic binding and groove bonds.

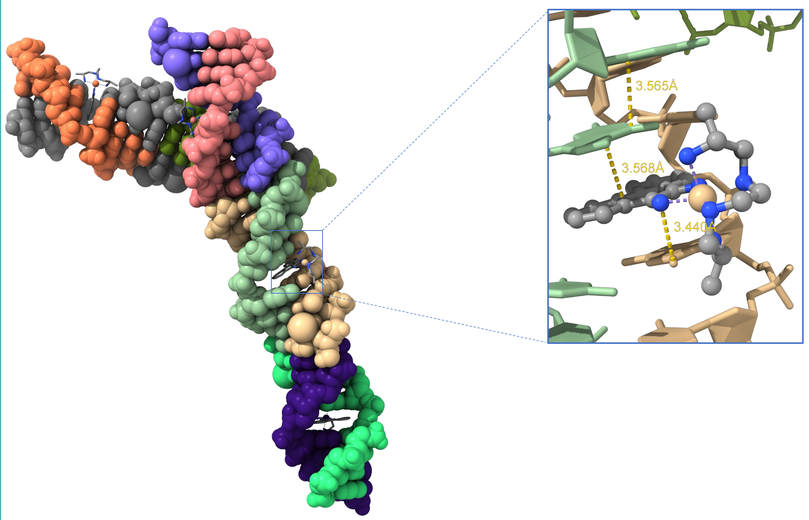

Figure 1. X-ray structure of the sequence-selective intercalation of $[Rh(Me_2trien)(phi)]^{3+}$ into the DNA sequence 5'-TGCA-3'. Sourced from PDB file 454D.

1. B. J. Pages, D. L. Ang, E. P. Wright, J. R. Aldrich-Wright, Dalton Trans., 2015,44, 3505-3526.
2. C. L. Kielkopf, K. E. Erkkila, B. P. Hudson, J. K. Barton, D. C. Rees, Nat. Struct. Mol. Biol., 2000, 7, 117–121.
3. E. R. Johnson, S. Keinan, P. Mori-Sánchez, J. Contreras-García, A. J. Cohen, W. Yang, J. Am. Chem. Soc. 2010 132 (18), 6498-6506.

RESULTS

Synthesized complex
$[Cu(dmbpy)Cl_2]$

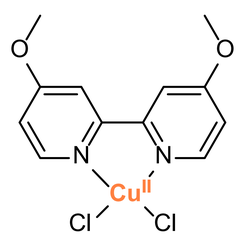

dmbpy = 4,4'-dimethoxy-2,2'-bipyridine

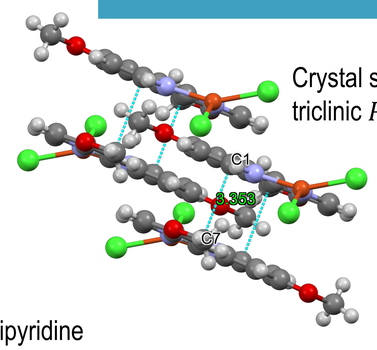

Crystal system:
triclinic $P\bar{1}$

In silico evaluation of biological activity of the ligand dmbpy and its Cu(II) complex.
We used the SwissTargetPrediction tool which allows to estimate the most probable macromolecular targets of a small bioactive molecules.

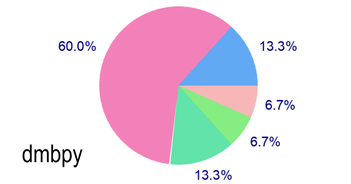

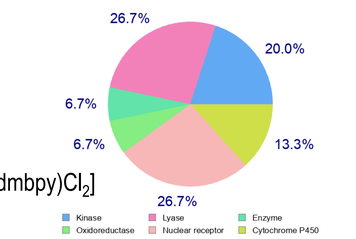

Spectroscopic characterization

Electronic structure of the Cu(II) complex

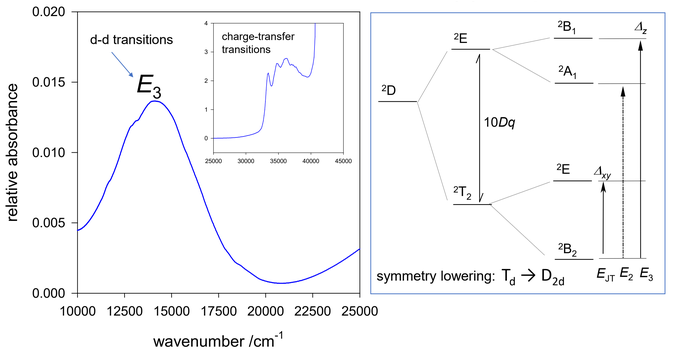

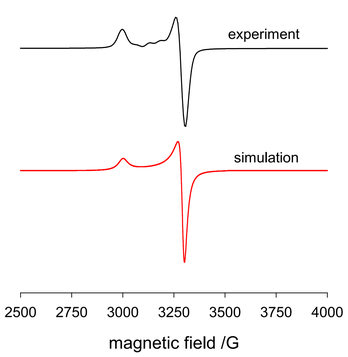

Spin-Hamiltonian parameters:

EPR data simulation
$g_{\parallel} = 2.25$
$g_{\perp} = 2.05$

DFT calculations
$g_x = 2.049$, $A_x = -16.6$ MHz
$g_y = 2.052$, $A_y = -27.7$ MHz
$g_z = 2.173$, $A_z = -527.2$ MHz

Complex – DNA interactions

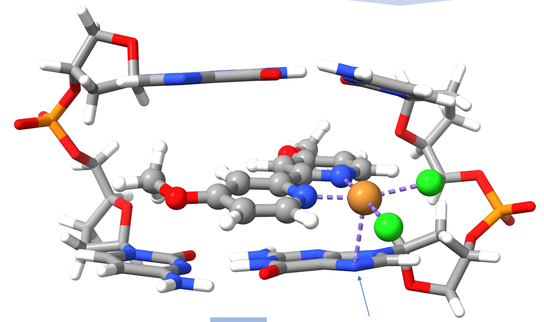

Two-layer B3LYP/XTB2 hybrid molecular dynamics simulation of the complex-DNA system

formation of a Cu-N7_G coordination bond

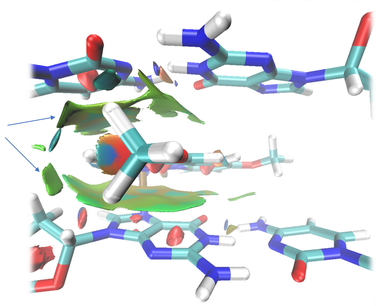

Studying weak interaction in complex-DNA system by NCI method based on promolecular density

Impact of different amendments on *Miscanthus* × *giganteus* biomass produced at the sustainably managed marginal and post-mining areas

UNIVERZITA J. E. PURKYNĚ V ÚSTÍ NAD LABEM
Fakulta životního prostředí

R.A. Newton [1*], **V. Pidlisnyuk** [1], **A. Mamirova** [1]

[1]Department of Environmental Chemistry and Technology, Faculty of Environment, Jan Evangelista Purkyně University, Pasteurova 15, Ústí nad Labem, 400 96, Czech Republic

INTRODUCTION

- The cultivation *of Miscanthus x giganteus* (*M×g*), a C4 perennial non-food crop, in the post-mining and post-military soils permits to improve the soil health, to reduce emission of greenhouse gases, and to produce sufficient amount of biomass.
- Cultivation of *M×g* on slightly contaminated or marginal soils offers environmental and economic advantages: the crop shows a sufficient remediation potential and is effective in carbon sequestration.
- When *M×g* is growing multiyear at such sites, the contaminants are mainly accumulated in the rhizomes thus the above ground biomass which has little or no contamination can be processed to fibrous and insulation materials, and packaging paper.
- The research aims to utilize *M×g* in the post-mining landscape when the soil has been amended by various amendments, to monitor the bio parameters, to study the change in soil nematode communities during multi-vegetation.

MATERIALS AND METHODS

- Growth parameters of *M×g* established in 2020 and 2021 (F2020 and F2021) on the former post-mining land in Chomutov, the Czech Republic, were assessed for three growing seasons for the F2020 and two growing seasons for the F2021. Monitored indicators included: the number of plants per plot, plant height, and biomass dry weight (DW) at harvest.
- Soil microbial and nematode communities were assessed for the F2021 during the first vegetation with a focus on nematodes. Soil samples to identify nematodes were collected three times during 2021: on 21 May - immediately after planting *M×g*, on 20 July - at mid-vegetation, and on 9 October - at the end of vegetation.

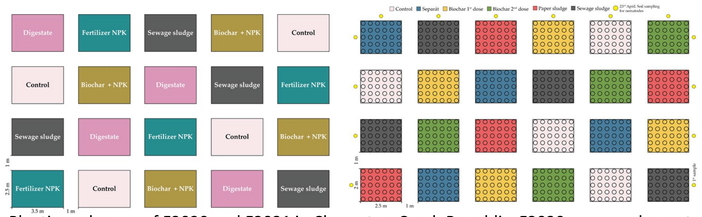

Planting schemes of F2020 and F2021 in Chomutov, Czech Republic. F2020 was supplemented with NPK, biochar + NPK (BNPK), digestate (D), and sewage sludge (SS). F2021 was supplemented with biochar in two dosages of 5 and 10% (BD1 and BD2), digestate (D), sewage sludge (SS), and hemicellulosic waste (HW).

Agrochemical parameters of the research soil.

Parameters	Unit	Value
pH (KCl)	-	4.9 ± 0.2
pH (H_2O)	-	5.7 ± 0.2
Organic matter	%	4.6 ± 0.3
Available P	mg kg^{-1}	50.6 ± 2.0
Available K	mg kg^{-1}	315 ± 9.8
Available Ca	mg kg^{-1}	1 769 ± 80.5
Available Mg	mg kg^{-1}	258 ± 7.3

Chemical content of the soil amendments.

Properties	Unit	Soil Amendments			
		BD	SS	D	HW
N	% DM	2.44 ± 0.03	2.99 ± 0.11	2.03 ± 0.07	5.51 ± 0.04
P	% DM	2.88 ± 0.03	1.98 ± 0.07	0.43 ± 0.01	0.90 ± 0.03
K	% DM	0.32 ± 0.03	0.22 ± 0.03	2.93 ± 0.07	0.75 ± 0.02
Ca	% DM	2.56 ± 0.06	2.19 ± 0.19	1.65 ± 0.23	4.47 ± 0.04
Mg	% DM	0.43 ± 0.02	0.45 ± 0.01	0.49 ± 0.05	0.32 ± 0.01
Na	% DM	0.19 ± 0.01	0.09 ± 0.01	0.24 ± 0.01	0.06 ± 0.01
Ash, 550 °C	%	69.1 ± 0.10	50.6 ± 1.20	36.2 ± 2.10	27.8 ± 0.20
C_{ox}	%	15.5 ± 0.01	24.7 ± 0.60	31.9 ± 1.00	36.1 ± 0.10
C:N	-	6.33 ± 0.07	8.26 ± 0.11	15.5 ± 0.74	6.55 ± 0.07

RESULTS

Height (cm) of *M×g* in various amended plots of F2020 over three vegetation. Different letters within a column indicate a significant difference between values.

Treatment	2020	2021	2022
Control	100 ± 5.0 **a**	234 ± 29.9	190 ± 8.4
NPK	62.9 ± 14.1 **c**	194 ± 41.8	170 ± 20.5
BNPK	69.5 ± 6.1 **bc**	195 ± 28.0	183 ± 21.5
D	84.5 ± 11.6 **ab**	232 ± 22.0	198 ± 9.9
SS	82.9 ± 5.6 **abc**	216 ± 37.2	183 ± 12.8
p-value	< 0.001	0.274	0.189

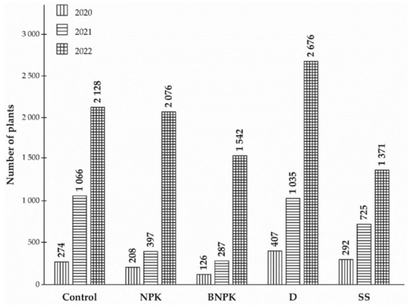

Total number of M×g plants in the various amended plots for the F2020

Height (cm) of M×g in various amended plots of F2021 over two vegetation.

Treatment	2021	2022
Control	109 ± 6.20	116.75 ± 5.56
BD1	100 ± 11.0	116.25 ± 29.04
BD2	105 ± 9.20	110.75 ± 10.47
D	106 ± 3.70	113.75 ± 2.06
SS	93.8 ± 3.60	100.00 ± 4.83
HW	106 ± 5.10	112.75 ± 5.32
p-value	0.0797	0.518

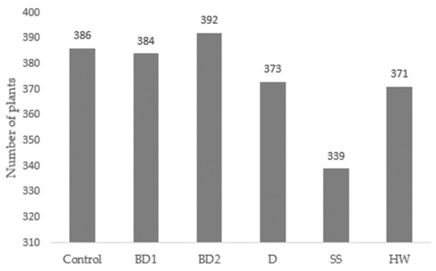

Total number of *M×g* plants in the various amended plots for the F2021 in 2022.

DW (kg) of *M×g* biomass harvested from F2020 in 2021, 2022 and 2023. Different letters within a column indicate a significant difference between values.

Treatment	Nov.2021	Nov.2022
Control	7.50 ± 1.20 **a**	7.76 ± 3.30 **a**
NPK	1.15 ± 0.05 **c**	2.45 ± 1.61 **b**
BNPK	2.35 ± 0.35 **bc**	2.79 ± 1.26 **b**
D	4.23 ± 0.55 **b**	6.38 ± 2.50 **a**
SS	3.2 ± 0.79 **b**	4.80 ± 3.30 **ab**
p-value	< 0.001	< 0.05

DW (kg) of *M×g* biomass harvested from F2021 in 2021 and 2022 . Different letters within a column indicate a significant difference between values.

Treatment	Nov.2021	Nov.2022
Control	0.11 ± 0.04 **b**	0.99 ± 0.39
BD1	0.15 ± 0.01 **ab**	1.27 ± 0.28
BD2	0.13 ± 0.01 **b**	0.85 ± 0.64
D	0.20 ± 0.02 **a**	0.72 ± 0.21
SS	0.09 ± 0.03 **b**	0.69 ± 0.09
HW	0.12 ± 0.02 **b**	0.66 ± 0.24
p-value	< 0.001	0.297

- The nematode community associated with crop establishment was sensitive to the type of amendments applied, which had a differential impact on the soil nematode food web. SS and D favored a more stable maturity status of the nematode community. The effects of BD1, BD2, and HW addition on nematodes were controversial.

CONCLUSIONS

- For F2020, the number of *M×g* in the plot supplemented with D was highest in the first and third vegetation, the highest biomass DW harvested in 2021 and 2022 was observed for the control plants. However, the highest biomass DW harvested in 2023 was observed for *M×g* in the plot supplemented with D.
- For F2021, the highest number of plants was recorded in the plot supplemented with BD2. After harvest in 2021, the DW of plants grown in soil amended with D was significantly higher than DW of plants grown in soil with other treatments except with BD1. There was no significance difference in the harvested DW in 2022 and 2023 of all plants grown in the different treatments.
- The nematode community structure was more mature for sewage sludge, less stable for digestate and had inconclusive effects for biochar and hemicellulose waste.

ACKNOWLEDGEMENTS

.

PLANT RNA VIRUS AS A TOOL FOR THE EXPRESSION OF FOREIGN POLYPEPTIDES IN PLANTS

ADAM ACHS[1], PETER ALAXIN[2], MIROSLAV GLASA[1,2], ZDENO ŠUBR[1]*

[1]Institute of Virology, Biomedical Research Center of the Slovak Academy of Sciences, Dúbravská cesta 9, 845 05 Bratislava, Slovakia
[2]Institute of Biology and Biotechnology, University of Ss. Cyril and Methodius, Námestie J. Herdu 2, 917 01 Trnava, Slovakia

INTRODUCTION

Expression vectors based on plant viral genomes provide a promising way of rapid, cost-effective and scalable production of recombinant proteins in plants. Plant viruses are infectious particles capable of autonomous replication and systemic spreading within their hosts. Given these unique features, plant viral replicons have been widely used for the expression of heterologous proteins in plants. Genomes of plant RNA viruses can be easily manipulated by a generation of infectious cDNA clones. Depending on the strategy of final host transfection, infectious transcripts or cDNA may be applied. Resultant infectious transcripts can be readily delivered to the target host plant either by direct mechanical inoculation or biolistic transfection. The biolistic method is applicable also for the infectious cDNA; however, *Agrobacterium*-mediated gene delivery is more favorable, allowing fast, simple, and efficient transient expression in plant tissues without the need for stable nuclear transformation. In our work, the expression vectors pAD/pAD-agro based on the plum pox virus (PPV) genome were used for the heterologous expression of different foreign polypeptides.

MATERIALS AND METHODS

The vector pAD consists of a full-length PPV-Rec cDNA under the control of the 35S CaMV promoter, cloned in the plasmid vector pGEM3. A cloning linker comprising EagI/KpnI restriction sites was introduced between the genes for viral replicase (NIb) and capsid protein (CP). The DAG motif-coding region within the CP essential for the aphid transmissibility of the virus was modified by site-directed mutagenesis. The vector pAD-agro was constructed by recloning the cDNA of PPV from pAD to the shortened commercial *Agrobacterium* binary vector pCambia 1304 (Abcam). Different genes of interest were either amplified by PCR or *de novo* synthetized using a commercial service (Eurofins Genomics). Each of target genes was inserted into the pAD/pAD-agro vectors either by restriction cloning or by using In-Fusion HD Cloning Kit (Takara). The pAD constructs were introduced into *Nicotiana benthamiana* plants by biolistic method using a common airgun. The pAD-agro constructs were delivered by agroinfiltration. Leaf or root samples were analyzed by Western blot using PPV- and foreign protein-specific antibodies. Genetic stability of each construct was verified by RT-PCR using primers spanning the insertion site. Selected proteins were purified by immobilized metal affinity chromatography (IMAC) using HisPur Cobalt Resin (Thermo Scientific).

AIM

- **Application of PPV-based expression vectors pAD/pAD-agro for the expression of different foreign polypeptides in *Nicotiana benthamiana* plants**
- **Affinity purification of target proteins from plant tissues**
- **Optimization of protein accumulation by their targeting to the apoplast**

RESULTS

In total, eight sequences originating from six foreign genes (one bacterial and five viral) were cloned into the pAD/pAD-agro vectors to evaluate their expression in *Nicotiana benthamiana*: alfalfa mosaic virus capsid protein (AMV CP), zucchini yellow mosaic virus capsid protein (ZYMV CP), the small heat-shock protein of *Cronobacter sakazakii* fused with hexahistidine (sHSP-his), a fragment of influenza A virus hemagglutinin (HA2-2), influenza A virus protein PB1-F2, SARS-CoV-2 nucleocapsid protein (CoN2-his), and its N- and C-terminal fragments (CoN-1-his and CoN3-his, respectively), each fused with a hexahistidine anchor. Particular proteins differed in their accumulation, tissue localization, stability, and solubility. The accumulation rate of produced polypeptides varied from low (N, hemagglutinin fragment) to relatively high (plant viral CPs, N-terminal fragment of N, PB1-F2). Some proteins preferentially accumulated in roots (sHSP, hemagglutinin fragment, PB1-F2), showing signs of proteolytic degradation in leaf tissues.

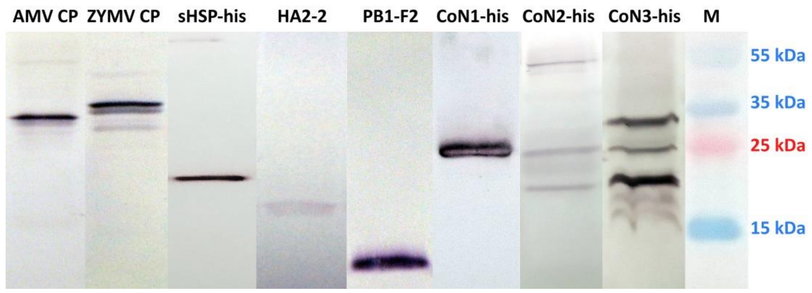

Fig. 1 Western blot analyses of particular proteins produced in *N. benthamiana*

Based on these results, CoN1-his was purified by IMAC under both native and denaturing conditions. Native IMAC resulted in insufficient elution of CoN1-his from the resin. Higher efficiency was observed under denaturing conditions (comparable if 8M urea or 6M Guanidine-HCl was used), giving a high purity product with a yield of approximately 78 µg/g of fresh leaf tissue (Fig.3). Chaotropic IMAC was also successful for CoN3-his in contrast to full-length CoN2-his which could not be so far purified due to low expression level and proteolytic degradation. Targeting foreign proteins to the apoplast has been proven to be an efficient way to improve their stability and accumulation in plant tissues. Our preliminary results show that the fusion of SSext signal peptide to the N-terminus of CoN3-his indeed significantly increased its accumulation in *N. benthamiana* leaves compared to CoN3-his alone (Fig.2). Moreover, enhanced stability improved its purification by IMAC in presence of 6M GuHCl. Thus, this approach may help to improve the production of foreign polypeptides using potyvirus-based vectors. Interestingly, CoN3his_SSext was not detected in the apoplastic fluid of infected leaves as expected, indicating its retention within the cell.

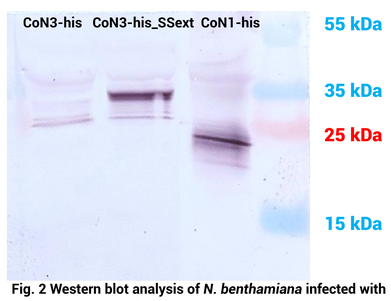

Fig. 2 Western blot analysis of *N. benthamiana* infected with pAD-agro_CoN3 and pAD-agro_CoN3-SSext constructs

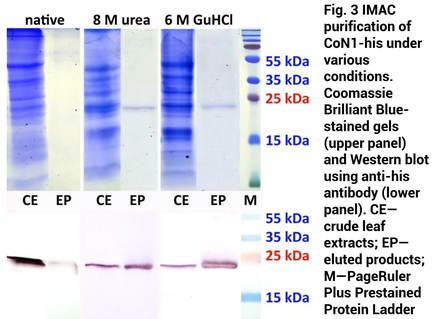

Fig. 3 IMAC purification of CoN1-his under various conditions. Coomassie Brilliant Blue-stained gels (upper panel) and Western blot using anti-his antibody (lower panel). CE—crude leaf extracts; EP—eluted products; M—PageRuler Plus Prestained Protein Ladder

CONCLUSIONS

- **Viral expression vectors pAD/pAD-agro are suitable for the production of different foreign polypeptides in *N. benthamiana,* however, each expression requires an individual approach concerning stability, solubility, or tissue localization, as these parameters may differ dramatically, depending on the cloned gene.**
- **Targeting expressed proteins to the apoplast may improve their stability. Despite higher accumulation levels, we were not able to confirm its secretion from the cell. Thus, further research has to be conducted to determine intracellular localization of targeted proteins.**

ACKNOWLEDGEMENTS

This work was supported by the grant 2/0003/22 from the Scientific Grant Agency of the Ministry of Education and Slovak Academy of Sciences (VEGA) and by the project APVV-20-0015 (Slovak Research and Development Agency).

REPEATED-BATCH PRODUCTION OF PHB BY *CUPRIAVIDUS NECATOR*

Ľ. JUREČKOVÁ, D. CHMELOVÁ, M. ONDREJOVIČ

Institute of Biology and Biotechnology, Faculty of Natural Sciences, University of Ss. Cyril and Methodius in Trnava, Slovakia

ABSTRACT

Cupriavidus necator bacteria are typical producers of polyhydroxybutyrate (PHB), which is the main representative of the polyhydroxyalkanoates (PHAs). The aim of this study was to evaluate selected fermentation conditions affecting the growth of the *C. necator* biomass as well as the intracellular accumulation of PHB by repeated-batch production. PHA accumulation by *C. necator* occurs most frequently in response to environmental stress conditions. Therefore, a two-stage cultivation consisting of cultivation in propagation medium aimed at maximizing biomass production and subsequent cultivation in production medium aimed at maximizing PHA production appears to be the most appropriate method. The repeated-batch fermentations were carried out in ten cycles in a bioreactor, obtaining a dry biomass yield ~6.4 g/L and a PHB yield determined by GC ~59.1 %, averaged over each cycle. This suggests the potential of *C. necator* biomass utilization in multiple cycles without the need to always inoculate the bacteria and reduce the cost of PHB production.

Up-stream

Production organism

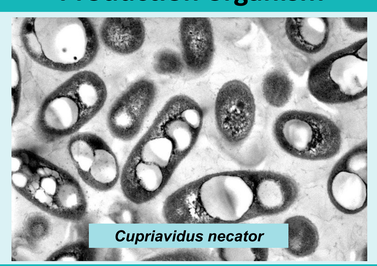

Cultivation medium

Nitrogen source

Phosphates

Carbon source

DIRECT USE

ENZYME TREATMENT

MICROBIAL TREATMENT

Optimization of the propagation and production medium

$$Y = b_0 + \sum_{i=1}^{k} b_i X_i + \sum_{i=1}^{k} b_{ii} X_i^2 + \sum_{\substack{i=1 \\ i<j}}^{k-1} \sum_{j=2} b_{ij} X_i X_j$$

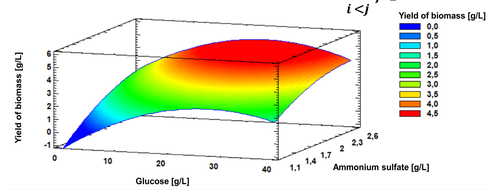

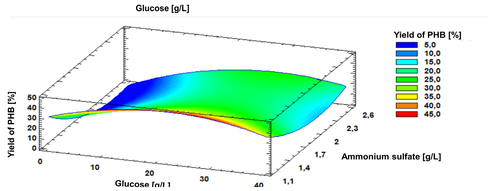

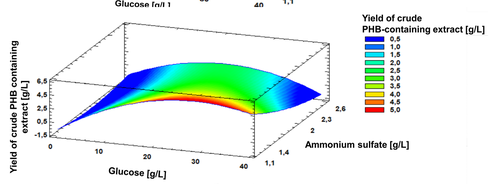

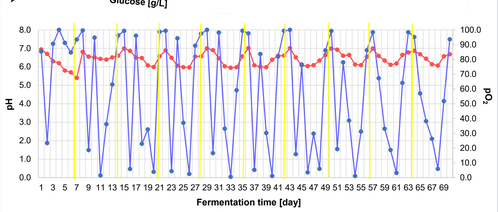

Two-stage fermentation

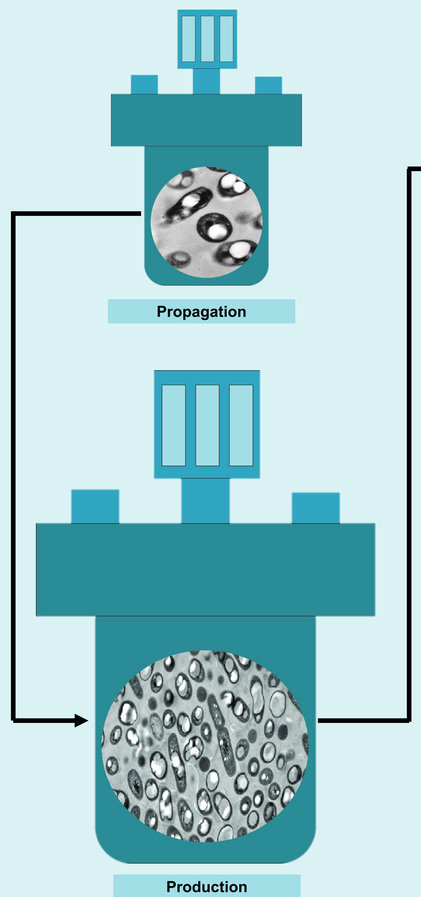

Down-stream

Isolation

Purity

Application

ACKNOWLEDGEMENTS

This work was supported by APVV-18-0420.

Morphological response of amaranth plants (*Amaranthus* spp.) to selected toxic metals

MONIKA LISINOVIČOVÁ[1,2]*, MONIKA SZABÓOVÁ[1], ANDREA HRICOVÁ[1]

(Presenting author is underlined, *corresponding author),

[1]Institution of Plant Genetics and Biotechnology, Plant Science and Biodiversity Centre, Slovak Academy of Sciences, Akademická 2, 950 07 Nitra, Slovakia

[2]Department of Plant Physiology, Faculty of Natural Sciences, Comenius University, Mlynská dolina, Ilkovičova 6, 842 15 Bratislava 4, Slovakia

INTRODUCTION

Amaranth (*Amaranthus* spp.) is a **pseudocereal** mainly used for edible leaves and seeds with **excellent nutritional properties**, which is one of the main reasons why it has attracted immense interest over recent years. It is a valuable alternative crop for easily cultivated, fast growing, high biomass production and **extraordinary adaptability** to adverse growing conditions, including excessive content of heavy metals (HMs) in soil.

HMs are not biodegradable, remain in ecosystems for a long time and enter the food chain. **Lead (Pb)** and **cadmium (Cd)** are elements that belong to **the most toxic** and most difficult to degrade HMs. Even in low concentrations, they might cause cytotoxic and mutagenic effects in plants, as well as **anatomical and morphological deformations** and **growth reduction**. Recently, the amaranth stress response to HM has been intensively investigated for **soil remediation strategies** in agriculture.

MATERIALS AND METHODS

Grain amaranth varieties: Slovak varieties 'Pribina' (*A. cruentus*) and 'Zobor' (*A. hypochondriacus x A. hybridus*), and commercial variety Plainsman (*A. hypochondriacus x A. hybridus*)

Hydroponic experiments: in a plant growth chamber (23°C, 16/8 light/dark cycle, 50% humidity)

The HMs: $Pb(NO_3)_2$ (200 mg/L) and $CdCl_2$ (15 mg/L)

Morphological measurements (Tab.1): biomass production during hydroponics (total FW in day 21 – total FW in day 0), root:shoot ratio

Determination of Cd and Pb uptake (Tab.2): ICP-OES

AIM

Our research was aimed at the following objectives:

- to describe the impact of HMs on selected growth parameters of amaranth,
- to establish the absorption and translocation rate of Cd and Pb,
- to determine the potential for phytoremediation of Cd and Pb in the tested varieties.

RESULTS

VARIETY	TREATMENT	BIOMASS INCREMENT	ROOT:SHOOT RATIO
'PRIBINA'	control	3.59 ± 1.69	1.39 ± 0.28
	Cd	1.97 ± 0.89	0.96 ± 0.12*
	Pb	0.05 ± 0.23*	0.61 ± 0.09*
'ZOBOR'	control	3.07 ± 1.55	0.89 ± 0.27
	Cd	0.68 ± 0.58*	0.60 ± 0.16
	Pb	0.30 ± 0.14*	1.40 ± 0.14*
PLAINSMAN	control	3.98 ± 0.40	1.52 ± 0.62
	Cd	0.23 ± 0.20*	0.71 ± 0.17
	Pb	-0.57 ± 0.35*	2.71 ± 0.15

Tab.1: Effect of Cd and Pb on growth parameters of three grain amaranth varieties (statistically significant differences in comparison to control plant tissues determined using t-test at $p < 0.05$ are marked with *).

VARIETY	TREATMENT	ROOT (mg/kg DW)	SHOOT (mg/kg DW)	TFRANSLOCATION FACTOR
'PRIBINA'	Cd	2016.37 ± 593.39*	466.92 ± 78.18*	0.25 ± 0.07*
	Pb	32922.65 ± 19805.78*	62.84 ± 31.69*	0.00 ± 0.00
'ZOBOR'	Cd	1331.91 ± 172.44*	107.13 ± 34.40*	0.08 ± 0.01*
	Pb	21201.19 ± 7250.70*	124.70 ± 146.05*	0.01 ± 0.05*
PLAINSMAN	Cd	1571.76 ± 306.30*	176.25 ± 58.51*	0.11 ± 0.02
	Pb	50686.93 ± 8514.97*	1929.45 ± 3331.17*	0.04 ± 0.06

Tab.2: The accumulation and translocation of Cd and Pb into root and shoot tissues of amaranth varieties (statistically significant differences in comparison to control plant tissues determined using t-test at $p < 0.05$ are marked with *).

CONCLUSIONS

Our results suggest following conclusions:

- ✓ the tested varieties could tolerate applied metal ions without lethal effect, but growth was reduced,
- ✓ the varieties were capable of absorbing a high level of Cd and Pb, predominantly in the roots, with limited root-to-shoot translocation,
- ✓ tested varieties can be used as potential phytostabilizers of Cd and Pb,
- ✓ the most tolerant variety to these toxic metals was 'Pribina'.

ACKNOWLEDGEMENTS

This work was supported by the Scientific Grant Agency VEGA, grant number 2/0013/22.

Alnus glutinosa and soil microbial community response to HCH contamination

Amirbekov A.[1], Vrchovecka S.[1], Riha.J[1],Petrik I.[2] ,Friedecky D.[3] ,Novak A.[2],Cernik M.[1] ,Hrabak P.[1] ,Sevcu A.[1,4]*

[1]Institute for Nanomaterials, Advanced Technologies and Innovation, Technical University of Liberec, Liberec, Czech Republic
[2]Institute of Experimental Botany, Palacký University Olomouc, Olomouc, Czech Republic
[3]Laboratory for Inherited Metabolic Disorders, Palacký University Olomouc, Olomouc, Czech Republic
[4]Faculty of Science, Humanities and Education, Technical University of Liberec, Czech Republic

INTRODUCTION

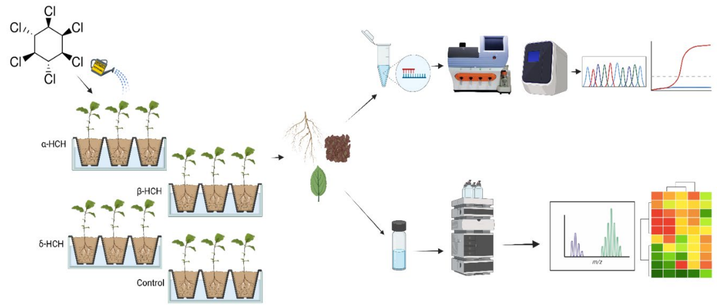

For this study, experimental substrates were prepared by mixing clean soil and standard α HCH, β HCH and δ HCH isomers to achieve 50 mg/kg dry weight of each, with a control soil sample prepared in the same way but without HCH.

MATERIALS AND METHODS

Chemical analysis

Prior to mixing the experimental substrates, the purity of the standard isomer solutions was assessed using an RSH/Trace 1310/TSQ8000 Gas chromatography–tandem mass spectrometry (GC-MS/MS) assembly with a DB-5ms column.

Hormone analysis was performed using an Acquity® I-Class ultra-high-performance liquid chromatograph coupled with a Xevo TQ-XS MS/MS assembly, using isotope dilution method as described by Šimura et. al, 2018.

DNA extraction and real-time quantitative PCR

DNA extraction of soil and rhizosphere samples was undertaken in duplicate using the DNeasy power Soil KIT. DNA yield and quality were then assessed using a Qubit fluorometer and agarose gel electrophoresis. QPCR analysis were performed to obtain CQ values of the selected genes and total bacterial biomass.

Amplicon 16S rRNA sequencing

The V4 region of the bacterial 16S rDNA gene was amplified, while for fungal abundance, the ITS2 region was amplified at a final volume of 50 µL.

The raw Ion Torrent reads were processed using QIIME 2 v.2021.8 software. Taxonomy was assigned to each amplicon sequence variant (ASV) using the q2-feature-classifier classifysklearn naive Bayes taxonomy classifier against the Silva 138 database, after which Mitochondria and Chloroplast were removed.

Statistical Analysis

The effect each HCH isomer on sapling growth parameters was evaluated using one-way ANOVA with post-hoc Tukey tests, using the Origin software package v.2019b (OriginLab Corporation, USA). Prior to analysis, all data were subjected to Levene's test to test for homogeneity of variance. All statistical analyses were performed with a significance level of $\alpha > 0.05$.

AIM

In this study, we aim to describe the uptake and transformation of HCH isomers by *A. glutinosa* saplings planted in freshly contaminated soil and compare the development of associated rhizosphere and soil microbial communities. In doing so, we also determine the physiological response of *A. glutinosa* to HCH isomers by measuring sapling biomass and phytohormonal activity.

RESULTS

Highest removal efficiency was observed in the group treated with β-HCH (90.26%), followed by α-HCH (64.85 %) and δ-HCH (57.08 %).

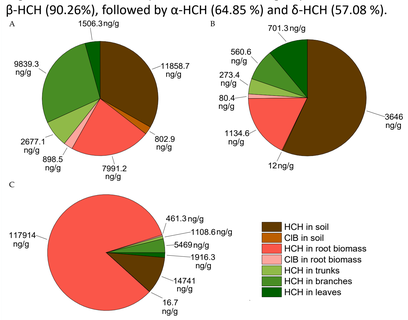

Concentrations of HCH isomers and metabolites (dry weight) in leaves, branches, roots and trunks of *A. glutinosa*. (A) α-HCH; (B) β-HCH; (C) δ-HCH.

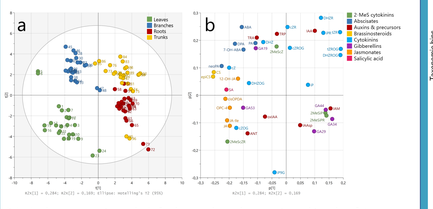

Principal components analysis for leaves, branches, roots and trunks of A. glutinosa. Scores (A) are given by concentration levels of phytohormones as loadings (B).

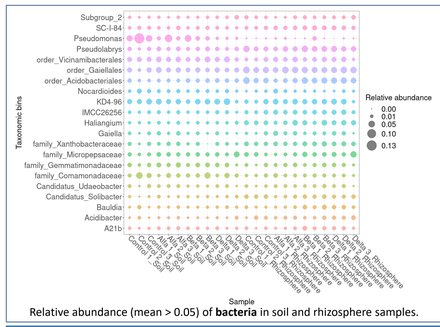

Relative abundance (mean > 0.05) of **bacteria** in soil and rhizosphere samples.

Soil and rhizosphere samples contained 530 common bacterial taxa and families. Of these, 93 species and families were found in the rhizosphere but not in the soil, 126 species and families in soil samples only. Soil bacterial community structure was similar in all samples treated with HCH. In soil samples, the dominant bacterial groups, in order, were Pseudomonas, the unclassified Chloroflexi group KD4-96, Comamonadaceae, Nocardioides and Gemmatimonadetes. While pseudomonas was dominant, with abundance levels highest in control samples, levels decreased noticeably in samples treated with HCH. *Pseudomonas* levels were significantly lower than in soil samples in all HCH treatments, with lowest abundance for the δ-HCH isomer, despite this being detected at highest levels in the root biomass.

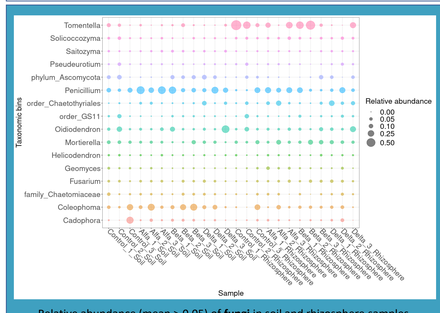

Relative abundance (mean > 0.05) of **fungi** in soil and rhizosphere samples.

Soil and rhizosphere samples contained 138 common fungal species and families, with 33 species and families found in the rhizosphere but not in soil and 86 species and families found only in soil samples. The abundance of Penicillium and Coleophoma was higher in the soil than in the rhizosphere, while levels of Moritella were higher in the rhizosphere. While Tomentella was generally dominant in rhizosphere samples, samples treated with δ-HCH had the lowest concentrations and β-HCH samples and the control the highest.

Table 1. Relative abundance of genes indicating total bacterial biomass (16S rDNA), dehydrochlorinase (linA), haloalkane dehalogenase (linB, linB-RT) and reductive dechlorinase (linD) in rhizosphere and soil samples (average of duplicate samples). The colour scale indicates the relative quantity of a given marker: red (+++) highest, orange (++) high, yellow (+) intermediate, (+-) low and ND = not detected or below the LOQ.

		gene				
		U16SRT	linA	linB	linB-RT	linD
Rhizosphere	Control 1	+++	+-	+-	+-	+-
	Control 2	+	ND	+-	+-	+-
	Control 3	+	+-	+-	+-	+-
	alpha 1	++	+-	+-	+-	+-
	alpha 2	++	+-	+-	+-	+-
	alpha 3	++	ND	+-	ND	+-
	beta 1	+++	ND	+-	+-	+-
	beta 2	+++	ND	+-	+-	+-
	beta 3	+++	+-	+-	+-	+-
	delta 1	++	ND	+-	+-	+-
	delta 2	+++	+-	+-	+-	+-
	delta 3	+	ND	+-	+-	+-
Soil	Control 1	+	+-	+++	ND	ND
	Control 2	+	+-	+-	ND	ND
	Control3	++	+-	+++	+-	+-
	alpha 1	++	+-	++	ND	+-
	alpha 2	++	+-	++	ND	ND
	alpha 3	+++	+-	+++	ND	ND
	beta 1	++	+-	++	+++	ND
	beta 2	++	+-	+++	+-	ND
	beta 3	+++	+-	+++	+++	+-
	delta 1	++	+-	+	NA	NA
	delta 2	+++	+-	+++	+-	NA
	delta 3	+++	+-	+	+-	NA

CONCLUSIONS

Owing to its physicochemical properties, the δ-HCH isomer was the most persistent in soils and the most strongly bound to A. glutinosa roots, with α-HCH the second major isomer recorded in soils treated with β-HCH and δ-HCH. All HCH isomers were found at highest proportions in the soil, with relatively little found in root biomass, suggesting that degradation of HCH isomers by bacteria in the soil occurs mainly through the upstream pathway. In rhizosphere bacteria, however, high amounts of the linD gene confirmed HCH degradation via downstream pathways. Overall, there was no significant difference in the abundances of bacterial and fungal consortia between treated and control samples. Similarly, there were no significant differences between soil and rhizosphere microorganisms. Phytohormone analysis indicated that A. glutinosa reacts to HCH contamination through changes in the stress hormones CK, JA, abscisate and GA. To conclude, A. glutinosa saplings showed clear uptake of all HCH isomers, with highest quantities detected in the roots and lowest in the leaves. While our pot experiment with freshly dissolved HCH isomer provide useful information about the potential of alder trees for phytoremediation, it is important to recognize the limitations of the experiment and the extent to which it can represent the real-life conditions.

ACKNOWLEDGEMENTS

This work was supported by the Student Grant Scheme at the Technical University of Liberec through Project no. SGS-2021-305, the EU Life Programme under the project LIFEPOPWAT (No. LIFE18 ENV/CZ/000374), the Ministry of Education, Youth and Sports of the Czech Republic (Project no. CZ.02.1.01/0.0/0.0/16_019/0000827) and through an Internal Grant of Palacký University Olomouc (IGA_PrF_2023_031).

GREEN ROOF SUBSTRATE AMENDMENT WITH SEWAGE SLUDGE BIOCHAR AND ITS EFFECT ON CHEMICAL LEACHING: A FIELD STUDY

MARTIN PIPÍŠKA[1], LENKA VAVRINCOVÁ[1,2], JANA URBANOVÁ[1] , VLADIMÍR FRIŠTÁK[1]

[1]Department of Chemistry, Faculty of Education, Trnava University in Trnava, Priemyselná 4, P.O. Box 9, Trnava, SK-918 43, Slovakia
[2]Department of Ecochemistry and Radioecology, Faculty of Natural Sciences, University of SS. Cyril and Methodius in Trnava, Nám. J. Herdu 2, Trnava, Slovakia

INTRODUCTION

Many studies have reported a positive effect of green roofs (GRs) on rainwater quality (Akther et al., 2020). The ability of GRs to retain rainwater and modify its quality depends mainly on the composition of the green roof substrate. Commonly used commercial substrates mainly use primary raw material sources and often do not take into account the local availability of substrate components. Therefore, it is interesting to find alternative components that allow recycling and reuse of waste materials, that are produced in huge quantities worldwide, such as nutrient-rich sewage sludge (SS) from wastewater treatment plants. In order to maintain the safety of roof substrates, appropriate treatment of the SS as substrate component becomes crucial. A promising strategy appears to be the pyrolytic transformation of SS to carbonized product (biochar). However, the environmental impact of addition of the SS biochar in roof substrate has not yet been thoroughly investigated, and therefore long-term monitoring of runoff water quality is required. In this work, SS biochar was applied as innovative additive to extensive green roof substrate at application rate 0, 10 and 20% (v/v) and its long-term impact on runoff quality was monitored on experimental green roof.

MATERIALS AND METHODS

In this study, commercial extensive green roof substrate (JV Intersad, Slovakia) was modified with SS biochar in application rate 0, 10 and 20% (v/v), and experimental green roof was established in October 2020 on a rooftop of the Faculty of Education of the University of Trnava (Fig. 1). Four replicates for each substrate mixture (SB0, SB10, and SB20) were planted with *Sedum* plug plants, and the runoff from each experimental platform was collected for water quality analysis. Routine analysis of pH, electrical conductivity (EC) and total dissolved solids (TDS) were determined using pH/EC/TDS multimeter and total suspended solids (TSS) using turbidimeter. Chemical oxygen demand (COD), total nitrogen (TN) and total phosphorus (TP) were analyzed spectrophotometrically after oxidizing in thermoreactor. Before Cd, Cu, Fe, Mn, Pb and Zn analysis using AAS, samples were digested with HNO_3 in the microwave digestion system.

Fig. 1. Experimental green roof setup.

RESULTS

Our results show that the application of SS biochar did not significantly affect pH, EC, TSS and COD of runoff water (Fig. 2). Higher EC and COD values in runoff from SB10 and SB20 compared to SB0 were observed only after the first precipitation events while fluctuating of pH and TSS values appears to be related to erosion and substrate degradation during the winter period. Both TN and TP concentrations in runoff were significantly higher after the first leaching, compared to the subsequent progression, suggesting that the substrates display first-flush behaviour. Overall, both TP and TN concentrations have decreased in runoff over 30 months of study and the addition of SS biochar at 10 and 20% application rates did not pose a greater risk of water contamination than the conventional extensive substrate.

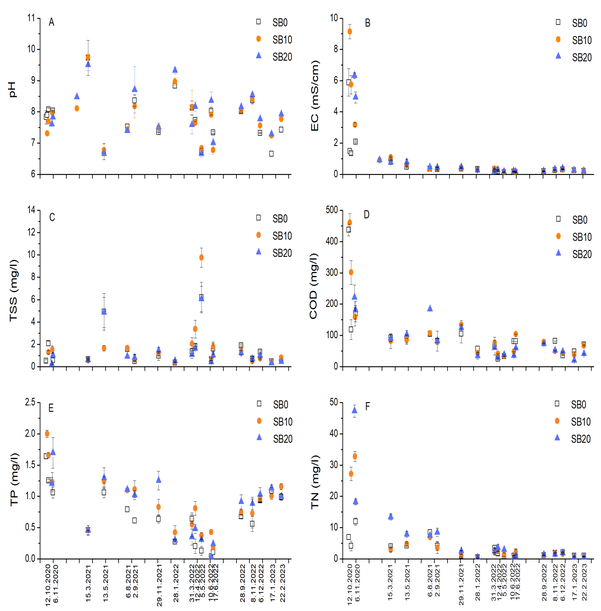

Fig. 2. Average (±SE) pH, EC, TSS, COD, and total phosphorus (TP) and total nitrogen (TN) concentrations in runoff from experimental green plots containing 8 cm of the substrate without biochar (SB0) and substrates with sewage sludge biochar (SB10 and SB20).

In spite of an increased concentrations of some metals (Cu, Pb, Zn) in the substrates with SS biochar, there were no significant differences in metal leaching between the substrates (Fig. 3). This result obviously confirms, that pyrolysis process leads to transformation of mobile forms of metals in sewage sludge into stable and relatively stable forms, and thus reducing their mobility. The first flush effect was typical for the leaching of each metal and we also noticed some other leaching trends during the studied period – lower pH of runoff led to higher leaching of Cu, Fe and Mn, and freeze-thaw cycles caused the leaching of Cd, Pb and Zn from eroded substrates. We should mention that the runoff from any substrate did not exceed the maximum metal concentrations for irrigation water according to US EPA and FAO guidelines.

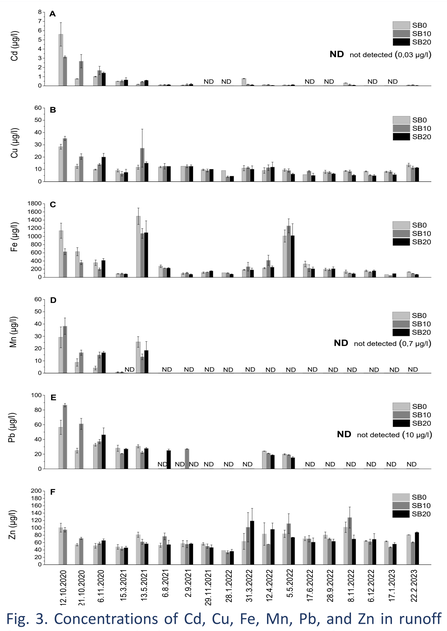

Fig. 3. Concentrations of Cd, Cu, Fe, Mn, Pb, and Zn in runoff from experimental plots containing 8 cm of the extensive substrate without biochar (SB0) and substrates with sewage sludge biochar (SB10 and SB20). Data represent the mean ± SE (n = 3-4). The absence of a column for a particulate substrate indicates that metal was below the detection limit.

CONCLUSIONS

Obtained results confirmed that the addition of SS biochar at 10 and 20% application rates does not significantly affect the pH, EC, TSS and COD of runoff water, does not pose a risk of water eutrophication, while beeing a good and long-term source of phosphorus for roof vegetation, and does not lead to excessive metals leaching. Based on our results, we suppose that sewage sludge-based biochar could be used as a valuable and water safe component of extensive substrates for green roofs.

REFERENCES

Akther et al. Ecol. Eng. 2020, 147, 105768.

Berndtsson, J.C. Ecol. Eng. 2010, 36, p. 351-360.

FAO Water quality for agriculture. 1985.

US EPA Guidelines for Water Reuse 600/R-12/618.

ACKNOWLEDGEMENTS

This research was funded by the Slovak Research and Development Agency under the contract number SK-AT-20-0004.

The Effects of Different Tree Species on Soil Properties and Soil Development

Lucie Buchbauerová[1*], Jan Frouz[1], Christian Lange[2], Fabio Vicentini[1]

(Presenting author is underlined, *corresponding author),

[1]Institute for Environmental Studies, Faculty of Science, Charles University, Benátská 2, 12801 Praha, CZ

[2]Forschungsinstitut für Bergbaufolgelandschaften e. V., Brauhausweg 2, 03238 Finsterwalde, DE

ÚŽP PřF UK

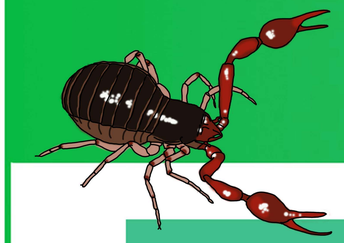

INTRODUCTION

According to common knowledge, there is a spectrum of ways of how the top soil layer (aka humus layer) develops. On one side of the spectrum, the leaf litter fallen from trees is degraded very slowly, and its unfinished layer becomes thicker. In this humus type, fungi are more prevalent than bacteria and the soil becomes acidic. On the other hand, there are cases and examples where the tree leaves are so quickly incorporated into the top soil layer that an unfermented and even fermented litter layer is almost absent. Bacteria are more common than fungi here and the soil usually becomes slightly alkaline.

Apart from microorganisms, soil fauna also plays a role in the speed with which leaf litter is decomposed and incorporated into the soil. The effect of trees on soil development is considered dependent on the quality of the leaves of the respective tree species. Leaf quality is then expressed as a ratio of carbon to nitrogen content, which suggests how easy are the leaves to decompose for organisms feeding on them.

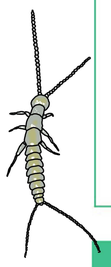

MATERIALS AND METHODS

The study site Domsdorf, which represents the spoil heaps around coal mine complex in Germany, is an overburden heap founded in the 1960s.

We measured the leaf nitrogen balance index (NBI, working off of fluorescence properties of the leaves) of trees growing on the spoil heaps: pine (*Pinus sylvestris*), birch (*Betula pendula*), red oak (*Quercus rubra*), sessile oak (*Quercus petraea*), lime (*Tilia cordata*), larch (*Larix decidua*), and alder (*Alnus glutinosa*), and performed phospholipidic fatty acids (PLFA, chemotaxonomic markers for soil microorganisms) analysis, pH measurement, measurement of nitrate content and carbon:nitrogen ratio in the soil under each tree species. Abundance of mesofauna and macrofauna was also counted in the samples from the ground beneath the trees using Arsenal stereomicroscope.

Within each stand, we chose three sampling spots, and after clearing the groud from leaf litter, we took samples from 0 and 10 cm below ground. For soil chemical properties, we used a metal cylinder with 10 cm in diameter and 10 cm in height to acquire the samples. For soil macrofauna analysis, we used identical cylinder. For taking mesofauna samples, we used three cylinders with 5 cm in diameter and 5 cm in height at each spot.

In order to obtain a polished soil profile for each spot, we used a metal rectangular thrusted to each soil profile.

AIM

- Forest reclamation is a very important issue of environmental studies, especially when considering human-affected sites such as coal mining areas.
Depending on which tree species is used for artificial afforestation of the spoil heaps, the recovery of the affected site can take different development paths and result in very different outcomes in terms of the quality of the final biotope.
Our research took place in the Lusatian mining area of Domsdorf, where we sought to sample reforested spoil heaps and compare the leaf litter and soil quality along with the abundance of the soil inhabitants between sites with several tree species.

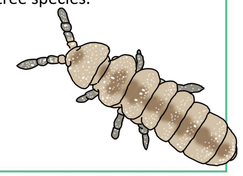

RESULTS

As our marker of choice to represent the leaf quality, the NBI was chosen. NBI proved to be high in red oak, lime and alder, while lower NBI was measured in pine, sessile oak and larch.

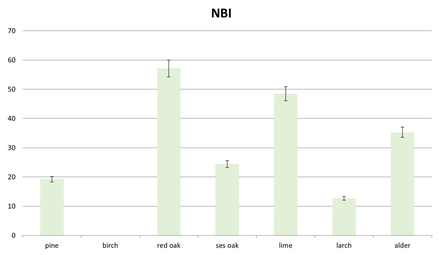

Nitrate content in the soil under respective tree specie. Within closer look, similarities can be perceived with the data shown for NBI.

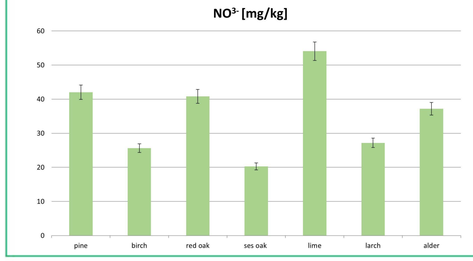

PLFA analysis showed that a high fungi:bacteria ratio exists in soils under pine and sessile oak. The lowest fungi:bacteria ratio was found in soils under birch, red oak, alder and larch, while the soil under lime presented an average fungi:bacteria ratio.

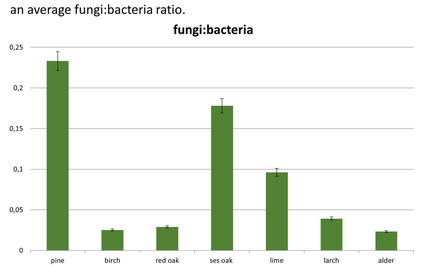

Soil macrofauna divided into ecological groups of predators and others (including detritovors, herbivors etc.)

Abundance for feeding strategies	Adults			Larvae		
	Sum	Predators	Others	Sum	Predators	Others
pine	62	51	11	7	1	6
birch	1	1		3	2	1
red oak	4	4		1		1
ses oak	15	11	4	1		1
lime	10	5	5	2		2
larch	6	2	4	1	1	
alder	3	2	1			

The numbers of specimens classified in four different taxonomic/ecological groups of mesofauna (pigmented springtails, not-pigmented springtails, oribatid mites and gamatid mites) varied under different tree species.

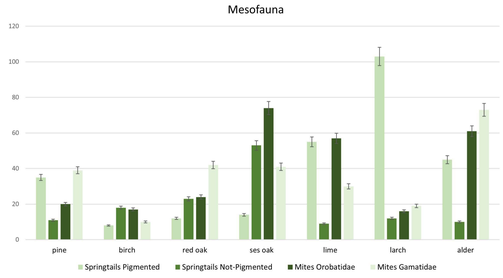

The pH values are lowest in pine and sessile oak, which corresponds to the low speed of soil development on these sites

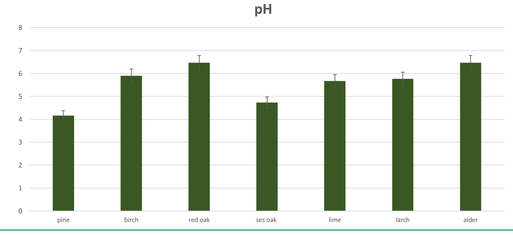

CONCLUSIONS

The heap spoils after coal mining can seem as an inhospitable environment. In this study, we attempted to look close at the importance of soil fauna-tree species (and their mutualistic symbionts) interactions, and with our results, we can support preexistent work emphasizing this importance.
The conditions ot the afforested study sites (for example the acidic properties of the original spoil substrate) have clearly been moderated by soil development processes, soil biota activity and decomposition of the leaf litter, over time – and the processes exhibit different speed under different tree species.

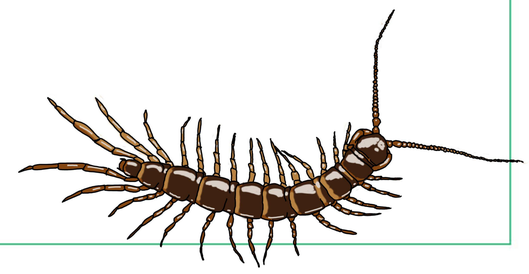

ACKNOWLEDGEMENTS

- Czech Science Foundation GAČR - GA13-110377S
Deutsche Bundesstiftung Umwelt